Infectious Disease Modelling 8 (2023) 1015–1031

Contents lists available at ScienceDirect

Infectious Disease Modelling

journal homepage: www.keaipublishing.com/idm

Mathematical modeling of malaria transmission dynamics in humans with mobility and control states

Gbenga Adegbite [a, b], Sunday Edeki [a, c], Itunuoluwa Isewon [a, b, e], Jerry Emmanuel [b, e], Titilope Dokunmu [a, d, e], Solomon Rotimi [a, d, e], Jelili Oyelade [a, b, e, *, 1], Ezekiel Adebiyi [a, b, e, f, 1]

[a] Covenant University Bioinformatics Research, Covenant University, Ota, Nigeria
[b] Department of Computer and Information Sciences, Covenant University, Ota, Nigeria
[c] Department of Mathematics, Covenant University, Ota, Nigeria
[d] Department of Biochemistry, Covenant University, Ota, Nigeria
[e] Covenant Applied Informatics and Communications-African Centre of Excellence, Covenant University, Ota, Ogun State, Nigeria
[f] Division of Applied Bioinformatics, German Cancer Research Center (DKFZ), Heidelberg, Germany

ARTICLE INFO

Article history:
Received 27 April 2023
Received in revised form 16 August 2023
Accepted 18 August 2023
Available online 21 August 2023
Handling Editor: Dr Yiming Shao

Keywords:
Malaria importation
Traditional malaria control
Ordinary differential equation
Quantitative properties
Novel algorithm
Runge-Kutta

ABSTRACT

Malaria importation is one of the hypothetical drivers of malaria transmission dynamics across the globe. Several studies on malaria importation focused on the effect of the use of conventional malaria control strategies as approved by the World Health Organization (WHO) on malaria transmission dynamics but did not capture the effect of the use of traditional malaria control strategies by vigilant humans. In order to handle the aforementioned situation, a novel system of Ordinary Differential Equations (ODEs) was developed comprising the human and the malaria vector compartments. Analysis of the system was carried out to assess its quantitative properties. The novel computational algorithm used to solve the developed system of ODEs was implemented and benchmarked with the existing Runge-Kutta numerical solution method. Furthermore, simulations of different vigilant conditions useful to control malaria were carried out. The novel system of malaria models was well-posed and epidemiologically meaningful based on its quantitative properties. The novel algorithm performed relatively better in terms of model simulation accuracy than Runge-Kutta. At the best model-fit condition of 98% vigilance to the use of conventional and traditional malaria control strategies, this study revealed that malaria importation has a persistent impact on malaria transmission dynamics. In lieu of this, this study opined that total vigilance to the use of the WHO-approved and traditional malaria management tools would be the most effective control strategy against malaria importation.

* Corresponding author. Covenant University Bioinformatics Research, Covenant University, Ota, Nigeria.
E-mail address: ola.oyelade@covenantuniversity.edu.ng (J. Oyelade).
Peer review under responsibility of KeAi Communications Co., Ltd.
[1] Joint Last authors.

https://doi.org/10.1016/j.idm.2023.08.005

1. Introduction

Malaria is a disease of concern in different countries of the World over the years (Girum et al., 2019; Narain & Nath, 2018). The greatest burden of the disease is carried by the Sub-Sahara African-residential human population according to recent reports (World Health Organization, 2018, 2020). However, the low socio-economic and educational status of most people that live in Africa are contributing factors to this burden (Darteh et al., 2021; Degarege et al., 2019; Ngandu et al., 2020). Also, climatic conditions such as wind, rainfall, relative humidity, and temperature; obtainable in Africa accelerate the survival and reproduction rate of the malaria vector (Adeola et al., 2017; Ngninpogni et al., 2021; Nkiruka et al., 2021). The *Plasmodium falciparum* specie is the predominant malaria infection parasite in the Sub-Sahara African region in contrast to other endemic regions of the World (Amambua-Ngwa et al., 2019; Kojom & Singh, 2020; Weiss et al., 2019).

Several control efforts in the Sub-Sahara African region have focused on curbing malaria by controlling the vector that serves as the primary host of the *Plasmodium* parasite (Beier et al., 2018, pp. 387–402; Benelli & Beier, 2017; Killeen et al., 2017). In line with this, the World Health Organization (WHO) has approved the use of conventional malaria vector control strategies such as Long Lasting Insecticide-treated Net (LLIN) and Indoor Residual Spray (IRS) (Kaindoa et al., 2021; Ryan et al., 2020; Syme et al., 2021). Asides from the WHO-approved malaria control strategies, a number of people in the Sub-Sahara African region employ the use of other common traditional malaria control strategies such as air conditioners, protective clothing, lotion, and house net (Bazan & Mora, 2020; Fischer, 2021; Shellvarajah et al., 2017). However, the effort to eliminate malaria by controlling the vector has not yielded the desired output in the past years as a result of the persistent issues of insecticide resistance and the high rate of non-adherence to the use of the malaria management tools by the human population (N'Do et al., 2021; Mekuriaw et al., 2020; Krezanoski et al., 2018). Hence, recent studies have focused on humans who serve as the secondary reservoir host for the malaria parasite. Specifically, most of these current clinical research studies investigated the factors responsible for malaria transmission using human subject reference data (Achieng et al., 2020; Anokye et al., 2018; Esayas et al., 2020). Several statistical and mathematical models have been useful in investigating these factors (Adeboye et al., 2020; Adegbite et al., 2022; Alegana et al., 2020; Li & Liu, 2020).

Mathematical models have specifically proven to be more useful than statistical models in studying the factors influencing the transmission dynamics of malaria because of their increased predictive computational capability (Li & Liu, 2020; Marshall et al., 2018; Sweilam et al., 2020). These models can be formulated using experimental data and biological knowledge (Awine et al., 2017; Marshall et al., 2018). Specifically, compartmentalized epidemiological mathematical model variants can be represented using continuous modeling constructs such as Ordinary Differential Equations (ODEs), Fractional Differential Equations, and the Partial Differential Equations (PDEs) (Almeida et al., 2021; Edeki et al., 2020; Handari et al., 2020; Tchoumi et al., 2021). In line with this, continuous models are constructed based on the conservation principle in mathematical biology (Brauer, 2017; Buonomo et al., 2018; Inaba, 2017). Models constructed based on conservation principle can be represented using different epidemiological incidence rates. Hence, the incidence rate could be bilinear, standard, and saturated depending on the size of the understudied population and the parameters of interest (Ahmed et al., 2018; Nana-Kyere et al., 2017).

Malaria importation is one of the hypothetical parametric factors influencing the dynamics of malaria transmission (Guerra et al., 2019; Iqbal et al., 2020; Mukhtar et al., 2020; Nana-Kyere et al., 2017). Malaria importation refers to the incidence of malaria infection in the human host in a new location due to prior travel to a malaria-endemic region (Chang et al., 2019; Iqbal et al., 2020). Specifically, malaria importation often occurs as a result of human travel from a high to low malaria transmission zone, as evident in several studies (Chang et al., 2019; Guerra et al., 2019; Iqbal et al., 2020; Mukhtar et al., 2020; Porter et al., 2020). In line with this, malaria importation could have an impact on malaria transmission dynamics. Hence, this study developed mathematical and computational models to study the effect of malaria importation as well as WHO-approved and traditional malaria control usage levels on malaria transmission dynamics using Covenant University environment which is a low malaria-endemic region in Nigeria, as case study (Adegbite et al., 2022). Furthermore, this study accounted for the hysteresis effect of the model based on the incubation period of *Plasmodium* infection in the human host. Hysteresis in malaria modeling is defined as the situation whereby the present state (malaria-infected condition) of an individual relies on its past (malaria-exposed) condition and other present condition (*Plasmodium* parasite incubation period in the exposed individual) (Schwinning et al., 2004; Yamana et al., 2017).

2. Materials and methods

2.1. Ethical permission

Ethical approval was acquired from the Covenant University Health Research Ethics Committee in carrying out this study (Ethical Registration No.:CU/HREC/AGA/157/22). This was because this study collected primary and secondary data from the human subjects on malaria. Furthermore, these primary and secondary data acquired for this study, were made to fulfill the bioinformatics standard of confidentiality. Informed consent was also gotten from the human participants prior to using their data for the research.

2.2. Study site and population

The Study site was the academic environment of Covenant University. Covenant University (Latitude 6.671823° N, Longitude 3.158125° E) is a Tertiary Institution located in Ota, which is a town in Ogun State very close to Lagos State, Nigeria (Adegbite et al., 2022). Specifically, the study site has a government-accredited Medical Centre that provides inpatient nd outpatient care services to the human population within the academic environment and in extension to people living in other parts of Ogun State (Adegbite et al., 2022). Ogun State is a State in the Southwestern part of Nigeria (Adegbite et al., 2022). *Plasmodium falciparum* parasite accounts for >95% of malaria–diagnosed cases in Southwestern Nigeria.

The study site consists of undergraduate and postgraduate students. The undergraduate students are fully residential within the School's academic environment, a controlled region where all the necessary vector control strategies are implemented. Hence, this study focused on studying malaria importation and the use of the conventional and traditional malaria control strategies among the undergraduate students residing in a low malaria transmission region. According to the University's Student Affairs Unit, the population strength of undergraduate students is approximately six thousand, one hundred and two (6102) as at the time of carrying out this study. In line with this, this study developed a mathematical model that can computationally predict the effect of malaria importation in tandem with the effect of the use of conventional and traditional control strategies; on malaria transmission dynamics within the understudied population of the project site.

2.3. The novel malaria mathematical model

In this study, we extended an existing Susceptible, Exposed, Infected and Recovery malaria transmission dynamics model in humans (Badshah & Akbar, 2021) into a new bilinear-incidence system of ODE(s) incorporating the Vigilant human class that use the conventional and traditional malaria control strategies (i.e. LLIN, IRS, air conditioner, protective clothing, house net, and lotion) as well as the Traveller and the Death compartments. Furthermore, we also included the female adult *Anopheles* mosquito population represented as Susceptible and Infected mosquito state variables in the model. The reason for the specific emphasis on the female *Anopheles* adult mosquito was because it is the gender variant responsible for malaria parasite infection transmission as a result of its contact with susceptible, infected and exposed human population as the case may be. The bilinear incidence rate was applied in this ODE-based system because the human population of interest was small (<10000) whereas the ODE continuous modeling construct was used because the population of interest was being studied from a homogenous point of view. The Undergraduate Students of Covenant University, Ota, Nigeria whose ages are between fifteen and twenty-two years ($15-22$) were the homogeneous human host population of interest in this study.

The model's development was based on the following assumptions.

i. Every human host has the same tendency to be exposed to malaria.
ii. Every human host has the same tendency to be infected with malaria

Fig. 1 showed the schematic flow diagram of the novel ODE-based malaria system.

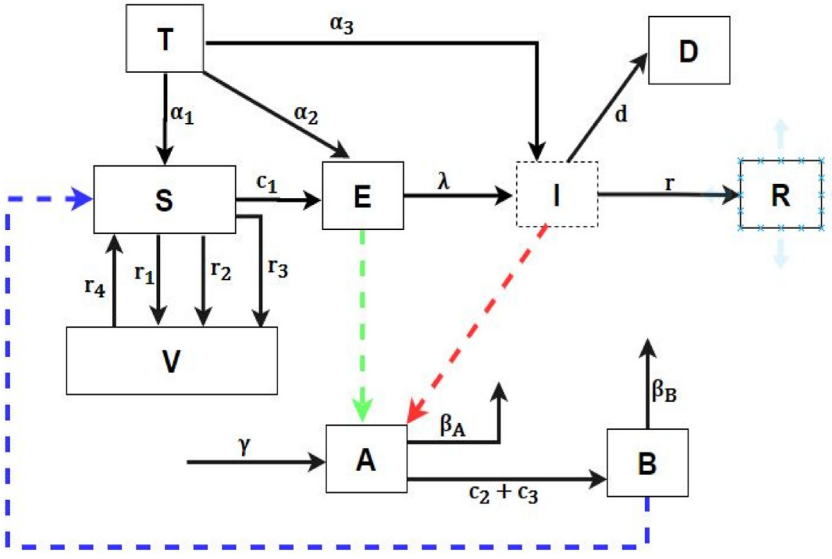

Fig. 1. Schematic Flow Diagram of the novel ODE-based System of Malaria.

The dotted and coloured lines in the diagram represent the different mechanisms (directions) of malaria infection transmission involving the malaria vector (female *Anopheles* mosquito) and the human host.

Based on the conservation and the mass action principles, we obtained the following ODE-based system represented using the bilinear incidence rate.

$$\left.\begin{aligned}
\frac{dT}{dt} &= -\alpha_1 T - \alpha_2 T - \alpha_3 T \\
\frac{dS}{dt} &= -r_1 S - r_2 S - r_3 S + \alpha_1 T + r_4 V - c_1 SB \\
\frac{dE}{dt} &= c_1 SB + \alpha_2 T - \lambda E \\
\frac{dI}{dt} &= \lambda E - Ir - Id + \alpha_3 T \\
\frac{dR}{dt} &= Ir \\
\frac{dD}{dt} &= Id \\
\frac{dV}{dt} &= r_1 S + r_2 S + r_3 S - r_4 V \\
\frac{dA}{dt} &= \gamma - \beta_A A - c_2 AE - c_3 AI \\
\frac{dB}{dt} &= c_2 AE + c_3 AI - \beta_B B
\end{aligned}\right\} \tag{1}$$

subject to the following initial conditions:

$$\left.\begin{aligned}
&T(0) > 0, S(0) > 0, E(0) > 0, V(0) > 0, \\
&I(0) = A(0) = B(0) = R(0) = D(0) = 0.
\end{aligned}\right\} \tag{2}$$

In the system of ODEs stated above, T is the human Traveller's Population variable, α_1 is the parameter representing the rate of influx of human Travellers into the Susceptible human Population of a given locality, α_2 is the parameter representing the rate of influx of the human Travellers into the human Exposed Population of a given locality, α_3 is the parameter representing the rate of influx of human Travellers into the human Infected Population of a given locality, S is the Susceptible human population variable, r_1 is the parameter representing the rate of use of LLIN, r_2 is the parameter representing the rate of use of IRS, r_3 is the parameter representing the rate of use of traditional malaria control strategies such as lotion, air conditioner, protective clothing and house net, r_4 is the parameter representing the rate of non-adherence to the use of the LLIN, IRS, air conditioner, lotion, protective clothing and house net, E is the Exposed human population variable, λ is the rate at which the exposed becomes infectious, I is the Infected human population variable, r is the recovery rate of the Infected Population as a result of treatment, d is the death rate of the Infected Population, R is the Recovered human population variable, D is the human Death population variable, V is the Vigilant human population variable, A is the Susceptible adult female *Anopheles* mosquito state variable, B is the Infected adult female *Anopheles* mosquito state variable, c_1 is the parametric constant representing the contact rate between the Susceptible human (S) and Infected *Anopheles* mosquitoes (B), c_2 is also the parametric constant representing the contact rate between the female Susceptible mosquito (A) and Exposed human (E) Population of a given locality, c_3 is the parametric constant representing the contact rate between the Susceptible mosquito (A) and infected human (I), γ is the recruitment rate of the female *Anopheles* mosquitoes, β_A is the mortality rate of the Susceptible female *Anopheles* mosquito (A) as a result of exposure to traditional and conventional vector control tools and β_B is the mortality rate of the Infected mosquito as a result of exposure to traditional and conventional vector control tools.

2.4. Numerical analyses of the novel malaria ODE-based system

An existing work by Imaga et al. (2022) proved beyond reasonable doubt the importance of checking for the existence and uniqueness of solution. In our own case, this was done using the Lipschitz continuity theorem.

Lipschitz Theorem Definition: Let D be a region such that (t, x_i) is the function's argument $f(.,.) = f(t, x_i), x_i \in X, t \geq 0$. Given any positive constant L, the function $f(x,t) = f\ (t,x)$ is said to satisfy Lipschitz condition if $|f\ (t,x_1) - f\ (t,x_2)| \leq L\ |x_1 - x_2| \nabla (t,x_1), (t,x_2) \in D$.

Prior to the application of the Lipschitz continuity condition, our developed system of mathematical models (1) was linearized and rewritten as follows.

$$\left.\begin{aligned}
&\frac{dT}{dt} = f_1(T) = -\alpha_1 T - \alpha_2 T - \alpha_3 T\\
&\frac{dS}{dt} = f_2(T,S,V,B) = -r_1 S - r_2 S - r_3 S + \alpha_1 T + r_4 V - c_1 SB\\
&\frac{dE}{dt} = f_3(T,S,E,B) = c_1 SB + \alpha_2 T - \lambda E\\
&\frac{dI}{dt} = f_4(T,E,I) = \lambda E - Ir - Id + \alpha_3 T\\
&\frac{dR}{dt} = f_5(I) = Ir\\
&\frac{dD}{dt} = f_6(I) = Id\\
&\frac{dV}{dt} = f_7(S,V) = r_1 S + r_2 S + r_3 S - r_4 V\\
&\frac{dA}{dt} = f_8(A,E,I) = \gamma - \beta_A A - c_2 AE - c_3 AI\\
&\frac{dB}{dt} = f_9(A,E,I,B) = c_2 AE + c_3 AI - \beta_B B\\
&T(0) > 0, S(0) > 0, E(0) > 0, V(0) > 0, I(0) = A(0) = B(0) = R(0) = D(0) = 0.
\end{aligned}\right\} \tag{3}$$

The region of interest (D) which contains all the model compartmental variables that we are interested in confirming their existence and uniqueness of solutions based on a Lipschitz constant, is given as follows.

$$\mathrm{D} = \left\{ \begin{array}{l} (T,S,E,I,R,D,V,A,B) : |T(t) - T(0)| \le a, |S(t) - S(0)| \le b,\\ |E(t) - E(0)| \le c, |I(t) - I(0)| \le d, |R(t) - R(0)| \le e, |D(t) - D(0)| \le f,\\ |V(t) - V(0)| \le g, |A(t) - A(0)| \le h, |B(t) - B(0)| \le i. \end{array} \right\} \tag{4}$$

Thereafter, the partial derivatives of each of the compartmental variables in system (3) were taken to obtain the following set of equations.

$$\left.\begin{aligned}
&\frac{df_1}{dT} = |-(\alpha_1 + \alpha_2 + \alpha_3)| \le |\alpha_1 + \alpha_2 + \alpha_3| < \infty, \frac{df_2}{dT} = |\alpha_1| < \infty,\\
&\frac{df_2}{dS} = |-r_1 - r_2 - r_3 - c_1 B| = |-(r_1 + r_2 + r_3 + c_1 B)| \le |r_1 + r_2 + r_3 + c_1 B| < \infty,\\
&\frac{df_2}{dV} = |r_4| < \infty, \frac{df_2}{dB} = |-c_1 S| \le |c_1 S| < \infty, \frac{df_3}{dT} = |\alpha_2| < \infty, \frac{df_3}{dS} = |c_1 B| < \infty,\\
&\frac{df_3}{dE} = |-\lambda| \le |\lambda| < \infty, \frac{df_3}{dB} = |c_1 S| < \infty, \frac{df_4}{dT} = |\alpha_3| < \infty, \frac{df_4}{dE} = |\lambda| < \infty,\\
&\frac{df_4}{dI} = |-r - d| = |-(r + d)| \le |r + d| < \infty, \frac{df_5}{dI} = |r| < \infty, \frac{df_6}{dI} = |d| < \infty,\\
&\frac{df_7}{dS} = |r_1 + r_2 + r_3| < \infty, \frac{df_7}{dV} = |-r_4| \le |r_4| < \infty, \frac{df_8}{dE} = |c_2 A| < \infty,\\
&\frac{df_8}{dI} = |-c_3 A| \le |c_3 A| < \infty,\\
&\frac{df_8}{dA} = |-\beta_A - c_2 E - c_3 I| = |-(\beta_A + c_2 E + c_3 I| \le |\beta_A + c_2 E + c_3 I| < \infty,\\
&\frac{df_9}{dE} = |c_2 A| < \infty, \frac{df_9}{dI} = |c_3 A| < \infty, \frac{df_9}{dA} = |c_2 E + c_3 I| < \infty,\\
&\frac{df_9}{dB} = |-\beta_B| \le |\beta_B| < \infty.
\end{aligned}\right\} \tag{5}$$

From the aforementioned derivations, the partial derivations (5) existed for every of the ODE-based models (3) and were continuous/bounded. Hence based on the Lipschitz continuity condition, the new system of ODE-based malaria models

possessed unique solutions at any given time variant. This further implies that the new system of malaria mathematical models in this study is meaningful and well-posed as desirable in mathematical epidemiology.

2.5. Positivity proof of the variables in the novel malaria ODE-based system

Some authors expatiated on the importance of proof of positivity to disease models (Edeki et al., 2020). Hence, we further quantified mathematically, if each of the variables in the novel ODE-based system of malaria in (1), satisfies the positivity condition. This was summarized briefly as follows:

In the system of mathematical models in (1), there are nine variables. As a case study, the positivity of the one of the nine variables in the system of ODE-based mathematical models which is T, was carried out using the following step-by-step methodology.

We applied separation of variables method on the ODE for compartment T in (1) as follows:

$$dT = -T(\alpha_1 + \alpha_2 + \alpha_3)dt$$

Further, we integrated both sides of the above equation.

$$\int_0^t dT = -T\int_0^t (\alpha_1 + \alpha_2 + \alpha_3)dt$$

$$\int_0^t \frac{dT}{T} = -\int_0^t (\alpha_1 + \alpha_2 + \alpha_3)dt$$

$$\ln T(t)|_0^t = -\int_0^t (\alpha_1 + \alpha_2 + \alpha_3)dt$$

$$\ln T(t) - \ln T(0) = -\int_0^t (\alpha_1 + \alpha_2 + \alpha_3)dt$$

Since $T(0) > 0$ then the equation was further written as follows based on the initial condition.

$$\ln T(t) = -\int_0^t (\alpha_1 + \alpha_2 + \alpha_3)\, dt$$

We took the exponential of both sides of the equation to confirm positivity.

$$e^{\ln T(t)} = e^{-\int_0^t (\alpha_1 + \alpha_2 + \alpha_3)\, dt}$$

$$\Rightarrow T(t) = e^{-\int_0^t (\alpha_1 + \alpha_2 + \alpha_3)\, dt} > 0$$

Hence, this proved that the variable T will always remain positive at any given time variant. The aforementioned step-by-step methodology applied to confirm the positivity of the T variable, were adapted to prove the positivity of the remaining variables S, E, I, R, D, V, A, B in the novel ODE-based malaria system. Hence, we concluded that S, E, I, R, D, V, A, B would all also remain positive at any given time-variant.

2.6. The novel algorithm for the mathematical model-based malaria prediction system

The system of equations in (1) can be re-defined as functions for $dT, dS, dE, dI, dR, dD, dV, dA, dB$ as follows:

$$\left.\begin{aligned}
functF^{T}(\,) &= (-\alpha_1 T - \alpha_2 T - \alpha_3 T)dt \\
functF^{S}(\,) &= (-r_1 S - r_2 S - r_3 S + \alpha_1 T + r_4 V - c_1 SB)dt \\
functF^{E}(\,) &= (c_1 SB + \alpha_2 T - \lambda E)dt \\
functF^{I}(\,) &= (\lambda E - Ir - Id + \alpha_3 T)dt \\
functF^{R}(\,) &= (Ir)dt \\
functF^{D}(\,) &= (Id)dt \\
functF^{V}(\,) &= (r_1 S + r_2 S + r_3 S - r_4 V)dt \\
functF^{A}(\,) &= (\gamma - \beta_A A - c_2 AE - c_3 AI)dt \\
functF^{B}(\,) &= (c_2 AE + c_3 AI - \beta_B B)dt
\end{aligned}\right\} \tag{6}$$

Hence, the novel algorithm for the implementation of a mathematical model-based malaria prediction system termed ModMTD was given as follows using compartment T as an example. $T_1, T_{15}, T_{30}, T_{45}, T_{60}, T_{75}, T_{90}, T_{105}, T_{120}$ denote the simulation value for T in 1 day, 15 days, 30 days, 45 days, 60 days, 75 days, 90 days, 105 days and 120 days, respectively.

Input: $T, \alpha_1, \alpha_2, \alpha_3$

Output: $T_1, T_{15}, T_{30}, T_{45}, T_{60}, T_{75}, T_{90}, T_{105}, T_{120}$

i. Initialize
$T_1 \leftarrow \{\}, T_{15} \leftarrow \{\}, T_{30} \leftarrow \{\}, T_{45} \leftarrow \{\}, T_{60} \leftarrow \{\}, T_{75} \leftarrow \{\}, T_{90} \leftarrow \{\}, T_{105} \leftarrow \{\}, T_{120} \leftarrow \{\}$

ii. Set $day_1 = \frac{1}{365}, day_{15} = \frac{15}{365}, day_{30} = \frac{30}{365}, day_{45} = \frac{45}{365}, day_{60} = \frac{60}{365},$
$day_{75} = \frac{75}{365}, day_{90} = \frac{90}{365}, day_{105} = \frac{105}{365}, day_{120} = \frac{120}{365}$

iii. While $(simul_{iteration} = 0, simul_{iteration} < 9, simul_{iteration}++)\, do$

iv. Call $functF^{T}()$

v. $T_1 = day_1 * dT, T_{15} = day_{15} * dT, T_{30} = day_{30} * dT, T_{45} = day_{45} * dT,$
$T_{60} = day_{60} * dT, T_{75} = day_{75} * dT,$
$T_{90} = day_{90} * \mathrm{d}T, T_{105} = day_{105} * dT, T_{120} = day_{120} * dT$

vi. End while

vii. Return $T_1, T_{15}, T_{30}, T_{45}, T_{60}, T_{75}, T_{90}, T_{105}, T_{120}$

Novel algorithms based on the specific ODE Function (F) for S, E, I, R, D, V, A, B in (6) were applied in this work similar to what was shown for compartment T. Furthermore, similar continuous time-point notations used to show the different outputs for compartment T were used for other compartmental algorithmic representations (S, E, I, R, D, V, A, B).

2.7. Model parameter estimation

This study estimated specifically the parameters representing the rate of use of traditional and conventional malaria control strategies and their respective non-adherence parametric rate based on the data obtained from the Undergraduate Students in Covenant University through the administration of questionnaires (likert scale) during the first week of resumption for a new academic session in September 2019. The model's initial variable condition for those that travelled was set to the total population count of Undergraduate Students in Covenant University as obtained from the Student Affairs Unit. This was because it is mandatory for all Undergraduate students to travel during the school's vacation periods. The model's variable initial condition for the Exposed was set based on the observed malaria incidence data obtained from the Covenant University Medical Centre (CUMC) during the first fourteen (14) days of resumption for a new academic session which was between September 15-29, 2019. The justification for the use of 14 days to derive the exposed (imported) initial simulation variable value was because the incubation period of *Plasmodium falciparum* in an exposed individual before the individual can become infectious is 14 days on the average. Also, the parameter representing the rate (probability) at which the exposed becomes infectious was set to be 1 because it is assumed that every exposed human will be recruited into the infected human population after the mandatory incubation period of *Plasmodium* infection in the human host. Based on the discussed parameter estimation methods used in determining the values for the Exposed initial simulation variable and the rate at which the exposed becomes infectious set in this work, hysteresis effect of the malaria model was taken into account.

Parameters such as the rates of influx of human Travellers into the Susceptible and Exposed human Population for our study area were set based on the aforementioned field data that was collected relating to the Traveller, Susceptible and Exposed Initial Variable Condition Values. Moreover, the parameter on the rate of influx of human Travellers into the Infected human Population for our study area was set based on the initial variable condition for the Infected human as this work assumed that it is not possible to determine the number of infected individuals at the model start state ($I(0) = 0$). This was also useful in accounting for the hysteresis effect of the model. In this study, some other parameters were also set based on information from literatures such as the rate of successful treatment (recovery), the death rate of individuals as a result of the malaria infection, recruitment rate of mosquitoes at different seasons, mortality rates of female *Anopheles* mosquitoes as a

result of use of malaria control tools as well as the contact rates between the female *Anopheles* mosquitoes and the human host (Ahkrizal et al., 2023; Arambepola et al., 2022; Arambepola et al., 2022, 2022; Collins & Duffy, 2022; Herdicho et al., 2021; Okuneye & Gumel, 2017; World Health Organization, 2020). Table 1a & 1b show the summary of the parameters used in this study with their definitions, values and data sources.

To derive the best model-fit scenario, this study assumed other possible conditions that can potentially reduce the impact of malaria importation by setting Vigilant human initial condition values to 80% and 98% of the total undergraduate human population (6102) as obtained from the student affairs unit of the University. These aforementioned new vigilant variables assumed in this study, denote the varying percentages of human host that were presumed to use traditional and conventional malaria control tools within the understudied population. For the two assumed vigilant conditions, only their floor values that are whole numbers, were used for the model simulations as human counts can not be in floating-point form.

2.8. Model simulation

A user-friendly computational tool was developed for model simulation using hypertext preprocessor (PhP), Javascript, Cascading Style Sheet, Hypertext Markup Language, Extensible Markup Language, MySQL Database, Asynchronous Javascript and Extensible Markup Language termed AJAX. The user's manual for using the software is provided in Appendix A. PhP technology was particularly useful in implementing the novel ODE-based algorithm.

2.9. Model performance evaluation

In this work, we checked preliminarily if any of the state variables of our model satisfies the Weierstrass approximation theorem. The Weisstrass approximation theorem states that for every exact solution, there is an approximate solution (Bond, 2009; Oghonyon et al., 2022). Further details as regards the Weierstrass Approximation theorem is given as follows.

Weierstrass Approximation Theorem Definition: Given that there is a real-valued function g with continuous time-point data (x,y) such that for every $\varepsilon > 0$, there must be an approximate value q (Bond, 2009; Oghonyon et al., 2022). Therefore, for all p in (x,y), there must be $|g(p) - q(p)| < \varepsilon$ where $|g(p) - q(p)|$ is the absolute error and ε is the tolerance level (convergence criteria) (Bond, 2009; Oghonyon et al., 2022).

Interpreting the theorem using simulation results from our different compartments, it is justifiable to say that only the infected human compartment satisfies this theorem because its exact values at different time points were gotten using empirically observed hospital-reported malaria cases while its approximate values were derived using the ModMTD algorithm and another numerical method of interest such as Runge Kutta during simulation. Other compartments in our developed novel system did not satisfy the Weierstrass approximation theorem as we do not have real data (exact solution) to compare with their respective simulation outputs (approximate solution) at different time points. Hence, we carried out performance evaluation of the novel algorithm developed in this study (ModMTD) with that of the existing Runge-Kutta numerical solution method with specific emphasis only on the Infected compartment.

Some authors discussed the prowess of using error estimation metrics such as absolute error, relative error, percentage error, absolute mean error and root mean square error as viable numerical accuracy testing tool for algorithms at continuous time-point intervals (Chutiman et al., 2021; Ndipmong & Udechukwu, 2022; Oghonyon et al., 2022). Hence, the implemented ModMTD algorithmic system was benchmarked with the existing Runge-Kutta numerical solution method with specific focus on the infected human compartment in oder to evaluate their accuracy using the aforementioned numerical testing tool (Abell & Braselton, 2022; Chutiman et al., 2021; Ndipmong & Udechukwu, 2022; Omoloye et al., 2022).

Table 1a
Some Parameters used in the work.

Parameters	Definition	Values	Sources
α_1	rate of influx of human Travellers into the Susceptible human Population.	0.965	Field data
α_2	rate of influx of the human Travellers into the human Exposed Population.	0.03	Field data
α_3	rate of influx of human Travellers into the human Infected Population.	0	Assumed
r_1	rate of use of LLIN.	0.320	Field data
r_2	rate of use of IRS.	0.1577	Field data
r_3	rate of use of traditional malaria control strategies such as lotion, air conditioner, protective clothing and house net.	0.099	Field data
r_4	rate of non-adherence to the use of LLIN, IRS, lotion, air conditioner, protective clothing and house net.	1.7326	Field data
c_1	contact rate between the Susceptible human (S) and Infected *Anopheles* mosquitoes (B).	0.0044	Okuneye & Gumel, 2017, Herdicho et al., 2021, Collins & Duffy, 2022
d	rate at which human dies as a result of infection.	0.00023	WHO, 2020
λ	rate at which the exposed becomes infectious.	1	Assumed
r	rate at which the infected recovers from the malaria disease after treatment.	0.99977	WHO, 2020

Table 1b
Other Parameters used in the work.

Parameters	Definition	Values	Sources
c_2	contact rate between the female Susceptible mosquito (A) and Exposed human (E).	0.0044	Okuneye & Gumel, 2017, Herdicho et al., 2021, Collins & Duffy, 2022
c_3	contact rate between the Susceptible mosquito (A) and Infected human (I).	0.0044	Okuneye & Gumel, 2017, Herdicho et al., 2021, Collins & Duffy, 2022
γ (dynamic based on seasons)	recruitment rate of the female *Anopheles* mosquitoes during high rain.	3500	Arambepola et al., 2022, Ahkrizal et al., 2023
γ (dynamic based on seasons)	recruitment rate of the female *Anopheles* mosquitoes during low rain.	875	Arambepola et al., 2022, Ahkrizal et al., 2023
β_A	mortality rate of the Susceptible female *Anopheles* mosquito (A) as a result of exposure to traditional and conventional vector control tools.	0.01	Ahkrizal et al. (2023)
β_B	mortality rate of the Infected mosquito as a result of exposure to traditional and conventional vector control tools.	0.01	Ahkrizal et al. (2023)

3. Results

Results from the implementation of the novel malaria algorithm incorporating the conventional and traditional malaria control strategies were presented. Results of the model's simulation using the acquired experimental data for the susceptible and vigilant human population at low and high rainy seasons were presented in Figs. 2 and 3, respectively Results of the model's simulation at 80% assumed vigilance to the use of traditional and conventional malaria control strategies during the low and high rainy seasons were presented in Figs. 4 and 5, respectively. Also, results of the model's simulation at 98% assumed vigilance to the use of traditional and conventional malaria control strategies during the low and high rainy seasons were presented in Figs. 6 and 7, respectively. We showed the initial simulation values for the variables and parameters and the different behaviours of all the different graphical displays for each of the compartments in our work. In order to enhance the interpretability of the model simulation outputs and handle the overlapping challenges in the graphing of some of the compartments, we presented the plotted data for all the compartments at the different simulation scenarios in Appendix B.

The results of the Comparative Performance Evaluation for the Model Simulations using ModMTD against hospital-observed Malaria Incidence data during high and low rainy seasons were presented in Tables 2 and 3, respectively with specific emphasis on the Infected compartment. Tables 4 and 5 show the results of the Comparative Performance Evaluation for the Model Simulations using Runge-Kutta algorithm against hospital-observed Malaria Incidence data during high and low rainy seasons, respectively; also with specific emphasis on the Infected compartment. Tables 6 and 7 show the comparative performance analysis between Runge-Kutta and ModMTD based on their absolute error values for low and high rain, respectively. Tables 8 and 9 show the comparative performance analysis between Runge-Kutta and ModMTD based on

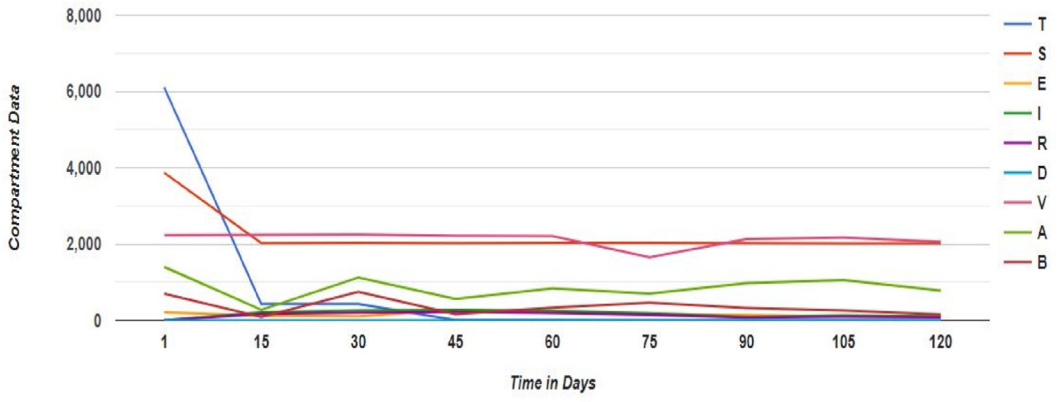

Fig. 2. Prediction Graph at low rain based on acquired experimental data
(Variable values $-\ c(T = 6102, S = 3869, V = 2233, E = 213, I = 0, R = 0, D = 0, A = 0, B = 0)$;
Parameters $-\ c(r_1 = 0.320, r_2 = 0.1577, r_3 = 0.099, r_4 = 1.7326, r = 0.99977, d = 0.00023, \gamma = 875, c_1 = 0.0044, c_2 = 0.0044, c_3 = 0.0044, \lambda = 1, \alpha_1 = 0.965, \alpha_2 = 0.03, \alpha_3 = 0, \beta_A = 0.01, \beta_B = 0.01)$)
Light-blue:Traveller that has an oscillatory behaviour, Orange:Susceptible which has an oscillatory behaviour, Yellow:Exposed that has an oscillatory behaviour, Green:Infected that has maximum followed by tailing off behaviour, Light-Violet:Vigilant that has an oscillatory behaviour, Violet:Recovered that has maximum followed by tailing off behaviour, Dark Blue:Death which has a linear behavior, Dark Violet: Infected mosquito that has an oscillatory behaviour, Light Green: Susceptible mosquito that has an oscillatory behaviour.

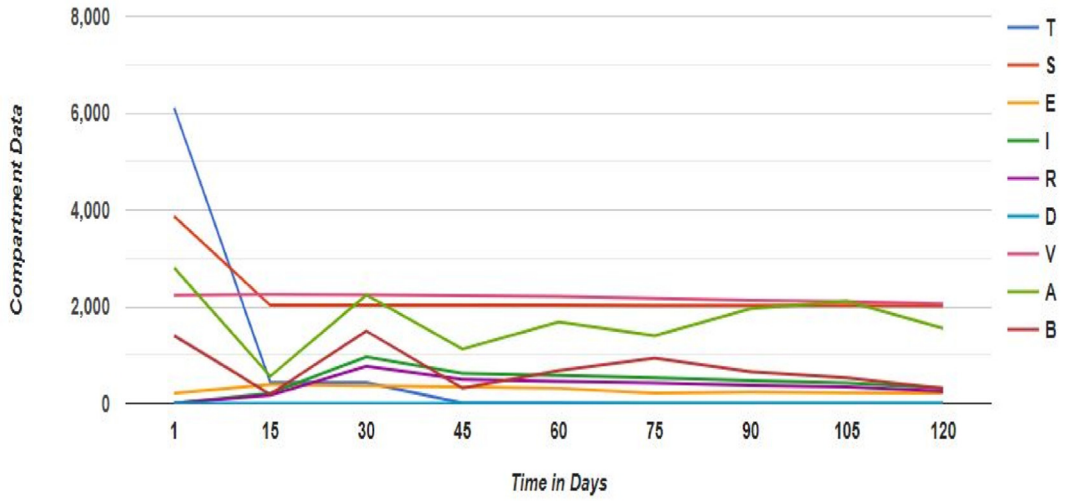

Fig. 3. Prediction Graph at high rain based on acquired experimental data
(Variable values $-\ c(T = 6102, S = 3869, V = 2233, E = 213, I = 0, R = 0, D = 0, A = 0, B = 0)$;
Parameters $-\ c(r_1 = 0.320, r_2 = 0.1577, r_3 = 0.099, r_4 = 1.7326, r = 0.99977, d = 0.00023, \gamma = 3500, c_1 = 0.0044, c_2 = 0.0044, c_3 = 0.0044, \lambda = 1, \alpha_1 = 0.965, \alpha_2 = 0.03, \alpha_3 = 0, \beta_A = 0.01, \beta_B = 0.01))$
Light-blue:Traveller that is decreasing to a limit, Orange:Susceptible which has an oscillatory behaviour, Yellow:Exposed that has an oscillatory behaviour, Green:Infected that has maximum followed by tailing off behaviour, Light-Violet:Vigilant that has an oscillatory behaviour, Violet:Recovered that has maximum followed by tailing off behaviour, Dark Blue:Death which has a linear behavior, Dark Violet: Infected mosquito that has an oscillatory behaviour, Light Green: Susceptible mosquito that has an oscillatory behaviour.

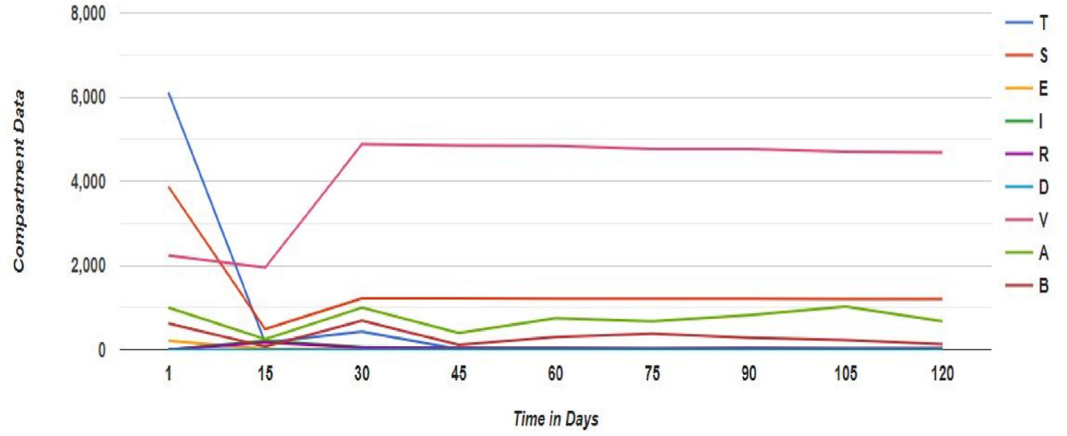

Fig. 4. Prediction Graph at 80% assumed vigilance during low rain
(Variable values $-\ c(T =)6102, S = 1220, V = 4881, E = 213, I = 0, D = 0, A = 0, B = 0$
Parameters $-\ c(r_1 = 0.320, r_2 = 0.1577, r_3 = 0.099, r_4 = 1.7326, r = 0.99977, d = 0.00023, \gamma = 875) c_1 = 0.0044, c_2 = 0.0044, c_3 = 0.0044, \lambda = 1, \alpha_1 = 0.965, \alpha_2 = 0.03, \alpha_3 = 0, \beta_A = 0.01, \beta_B = 0.01))$
Light-blue:Traveller that has an oscillatory behaviour, Orange:Susceptible which has an oscillatory behaviour, Yellow:Exposed that has an oscillatory behaviour, Green:Infected that has maximum followed by tailing off behaviour, Light-Violet:Vigilant that has an oscillatory behaviour, Violet:Recovered that has an oscillatory behaviour, Dark Blue:Death which has a linear behavior, Dark Violet: Infected mosquito that has an oscillatory behaviour, Light Green: Susceptible mosquito that has an oscillatory behaviour.

their relative error values for high and low rain, respectively. Tables 10 and 11 show the comparative performance analysis between Runge-Kutta and ModMTD based on their percentage error values for high and low rain, respectively The simulation scenario covered only time-series data from 15 to 60 days during high and low rainy periods because we took into account, different holiday periods specific to Covenant University which can hinder the students from staying longer than 60 days on campus. In the presented results in the different tables and graphs used to capture the data about the evaluation, $\text{Approx}_{\text{MTD}}$ represents the different model simulation values derived at different time-points (days) when the ModMTD algorithm was implemented, $\text{Exact}_{\text{OBS}}$ represents the hospital-observed malaria incidence data at different time intervals and $\text{Approx}_{\text{RK}}$ represents the different model simulation values derived at different time-points (days) when the Runge-Kutta algorithm was

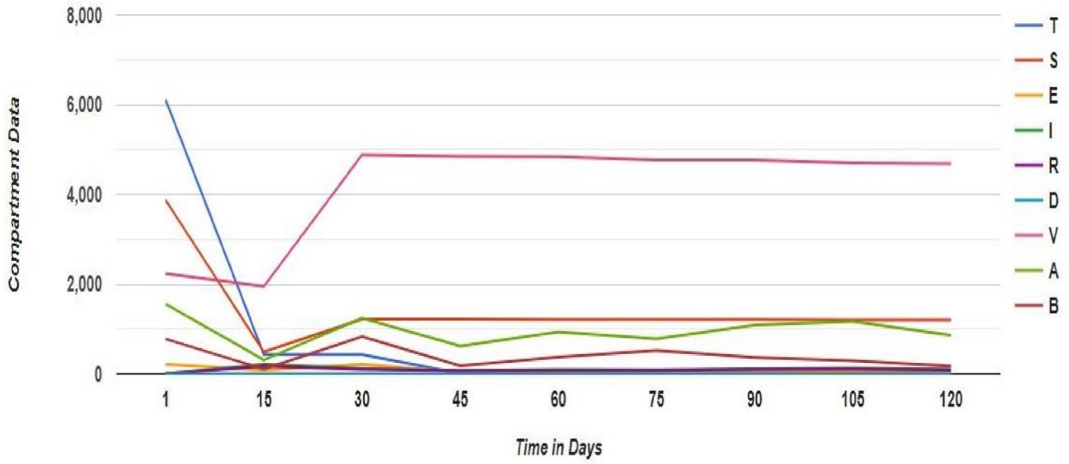

Fig. 5. Prediction Graph at 80% assumed vigilance during high rain
(Variable values $-\ c(T = 6102, S = 1220, V = 4881, E = 213, I = 0, R = 0, D = 0, A = 0, B = 0)$;
Parameters $-\ c(r_1 = 0.320, r_2 = 0.1577, r_3 = 0.099, r_4 = 1.7326, r = 0.99977, d = 0.00023, \gamma = 3500, c_1 = 0.0044, c_2 = 0.0044, c_3 = 0.0044, \lambda = 1, \alpha_1 = 0.965, \alpha_2 = 0.03, \alpha_3 = 0, \beta_A = 0.01, \beta_B = 0.01)$
Light-blue:Traveller that is an oscillatory behaviour, Orange:Susceptible which has an oscillatory behaviour, Yellow:Exposed that has an oscillatory behaviour, Green:Infected that has an oscillatory behaviour, Light-Violet:Vigilant that has an oscillatory behaviour, Violet:Recovered that has maximum followed by tailing off behaviour, Dark Blue:Death which has a linear behavior, Dark Violet: Infected mosquito that has an oscillatory behaviour, Light Green: Susceptible mosquito that has an oscillatory behaviour.

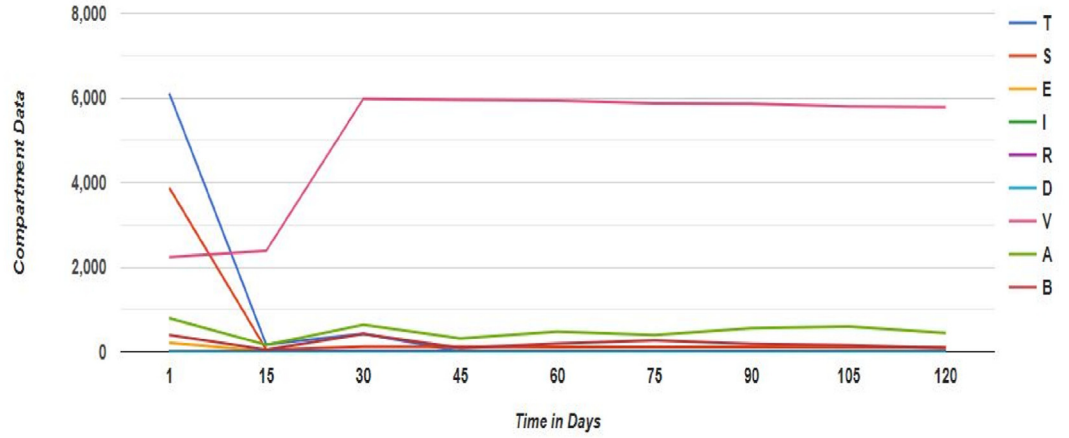

Fig. 6. Prediction Graph at 98% assumed vigilance during low rain
(Variable values $-\ c(T = 6102, S = 122, V = 5979, E = 213, I = 0, R = 0, D = 0, A = 0, B = 0)$
Parameters $-\ c(r_1 = 0.320, r_2 = 0.1577, r_3 = 0.099, r_4 = 1.7326, r = 0.99977, d = 0.00023, \gamma = 875, c_1 = 0.0044, c_2 = 0.0044, c_3 = 0.0044, \lambda = 1, \alpha_1 = 0.965, \alpha_2 = 0.03, \alpha_3 = 0, \beta_A = 0.01, \beta_B = 0.01)$
Light-blue:Traveller that that has an oscillatory behaviour, Orange:Susceptible which has an oscillatory behaviour, Yellow:Exposed that has an oscillatory behaviour, Green:Infected that has an oscillatory behaviour, Light-Violet:Vigilant that has an oscillatory behaviour, Violet:Recovered that has an oscillatory behaviour, Dark Blue:Death which has a linear behavior, Dark Violet: Infected mosquito that has an oscillatory behaviour, Light Green: Susceptible mosquito that has an oscillatory behaviour.

implemented. ABS_{ERR}, REL_{ERR}, and PER_{ERR} represent the absolute error, relative error and percentage error, respectively. Specifically ABS_{RK} and ABS_{MTD} represent the absolute error rates for Runge-Kutta and ModMTD, respectively. Also REL_{RK} and REL_{MTD} represent the relative error rates for Runge-Kutta and ModMTD, respectively. Furthermore, PER_{MTD} and PER_{RK} represent the percentage error rates for ModMTD and Runge-Kutta, respectively.

The Mean Absolute Error (MAE) Values when the ModMTD algorithm was used for model simulation during high and low rain were 2.0 and 1.0, respectively. Also the Root Mean Square Error (RMSE) when the ModMTD algorithm was used for model simulation during high and low rain were 3.74 and 1.22, respectively.

The MAE Values when the Runge-Kutta algorithm was used for model simulation during high and low rain were 3.5 and 2,0, respectively. Also the RMSE when the Runge-Kutta algorithm was used for model simulation during high and low rain

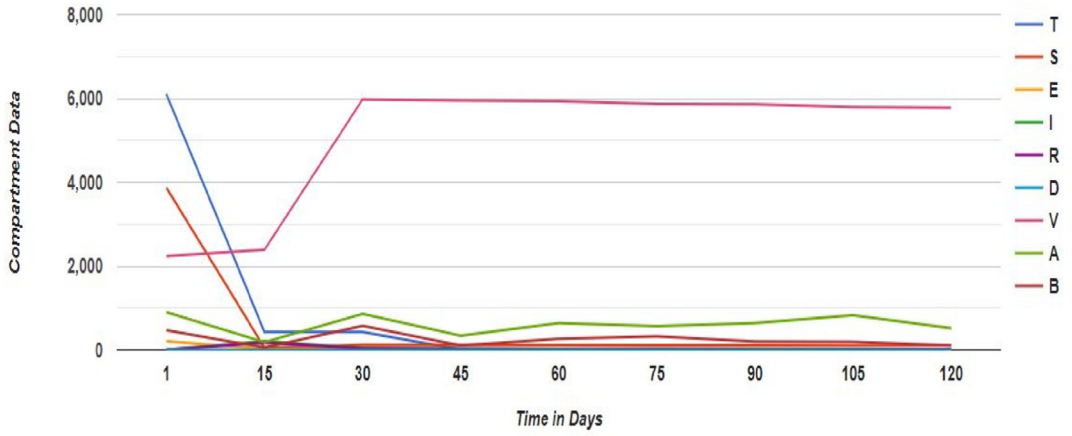

Fig. 7. Prediction Graph at 98% assumed vigilance during high rain
(Variable values $-$ c($T = 6102, S = 122, V = 5979, E = 213, I = 0, R = 0, D = 0, A = 0, B = 0$)
Parameters $-$ $c(r_1 = 0.320, r_2 = 0.1577, r_3 = 0.099, r_4 = 1.7326, r = 0.99977, d = 0.00023, \gamma = 3500, c_1 = 0.0044, c_2 = 0.0044, c_3 = 0.0044, \lambda = 1, \alpha_1 = 0.965, \alpha_2 = 0.03, \alpha_3 = 0, \beta_A = 0.01, \beta_B = 0.01)$)
Light-blue:Traveller that is decreasing to a limit, Orange:Susceptible which has an oscillatory behaviour, Yellow:Exposed that has an oscillatory behaviour, Green:Infected that has an oscillatory behaviour, Light-Violet:Vigilant that has an oscillatory behaviour, Violet:Recovered that has an oscillatory behaviour, Dark Blue:Death which has a linear behavior, Dark Violet: Infected mosquito that has an oscillatory behaviour, Light Green: Susceptible mosquito that has an oscillatory behaviour.

Table 2
Comparative Performance Evaluation for the Model Simulations using ModMTD against hospital-observed Malaria Incidence data during high rain.

Simulation in days	$Approx_{MTD}$	$Exact_{OBS}$	ABS_{ERR}	REL_{ERR}	PER_{ERR}
15	213	213	0	0	0
30	959	960	1	0.001	0.1
45	617	615	2	0.003	0.3
60	575	580	5	0.009	0.9

Table 3
Comparative Performance Evaluation for the Model Simulations using ModMTD and hospital-observed Malaria Incidence data during low rain.

Simulation in days	$Approx_{MTD}$	$Exact_{OBS}$	ABS_{ERR}	REL_{ERR}	PER_{ERR}
15	213	213	0	0	0
30	258	260	2	0.008	0.8
45	273	272	1	0.004	0.4
60	249	250	1	0.004	0.4

Table 4
Comparative Performance Evaluation for the Model Simulations using Runge-Kutta and observed Malaria Incidence during high rain.

Simulation in days	$Approx_{RK}$	$Exact_{OBS}$	ABS_{ERR}	REL_{ERR}	PER_{ERR}
15	213	213	0	0	0
30	958	960	2	0.002	0.2
45	620	615	5	0.008	0.8
60	573	580	7	0.01	0.1

Table 5
Comparative Performance Evaluation for the Model Simulations using Runge-Kutta and observed Malaria Incidence during low rain.

Simulation in days	$Approx_{RK}$	$Exact_{OBS}$	ABS_{ERR}	REL_{ERR}	PER_{ERR}
15	213	213	0	0	0
30	256	260	4	0.02	2.0
45	270	272	2	0.007	0.7
60	248	250	2	0.008	0.8

Table 6
Comparative Performance Evaluation of the Absolute Error Rate for the Model Simulations using Runge-Kutta and ModMTD during low rain.

Simulation in days	ABS_{RK}	ABS_{MODMTD}
15	0	0
30	4	2
45	2	1
60	2	1

Table 7
Comparative Performance Evaluation of the Absolute Error Rate for the Model Simulations using Runge-Kutta and ModMTD during high rain.

Simulation in days	ABS_{RK}	ABS_{MODMTD}
15	0	0
30	2	1
45	5	2
60	7	5

Table 8
Comparative Performance Evaluation of the Relative Error Rate for the Model Simulations using Runge-Kutta and ModMTD during high rain.

Simulation in days	REL_{RK}	REL_{MODMTD}
15	0	0
30	0.2	0.7
45	0.8	0.3
60	0.1	0.9

Table 9
Comparative Performance Evaluation of the Relative Error Rate for the Model Simulations using Runge-Kutta and ModMTD during low rain.

Simulation in days	REL_{RK}	REL_{MODMTD}
15	0	0
30	0.02	0.008
45	0.007	0.004
60	0.008	0.004

Table 10
Comparative Performance Evaluation of the Percentage Error Rate for the Model Simulations using Runge-Kutta and ModMTD during high rain.

Simulation in days	PER_{RK}	PER_{MODMTD}
15	0	0
30	0.1	0.001
45	0.008	0.005
60	0.01	0.009

Table 11
Comparative Performance Evaluation of the Percentage Error Rate for the Model Simulations using Runge-Kutta and ModMTD during low rain.

Simulation in days	PER_{RK}	PER_{MODMTD}
15	0	0
30	2.0	0.8
45	0.7	0.4
60	0.8	0.4

were 4.42 and 2.45, respectively. Figs. 8 and 9 show the graphs comparing the absolute error of $Approx_{MTD}$ with that of $Approx_{RK}$ during high and low rain, respectively. In the graphs, the first, second, third and 4th continuous time-points represent 15, 30, 45, and 60 days, respectively. The reason for showing the graph for ABS_{ERR} only is because its primary data was used in determining other error rates such as REL_{ERR}, PER_{ERR}, MAE and RMSE.

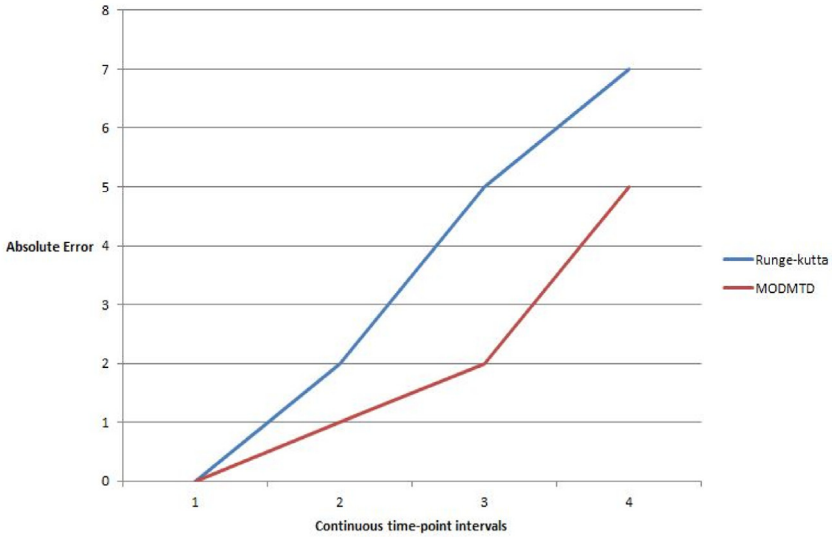

Fig. 8. The Absolute error rates for ModMTD and Runge-Kutta at high rain.

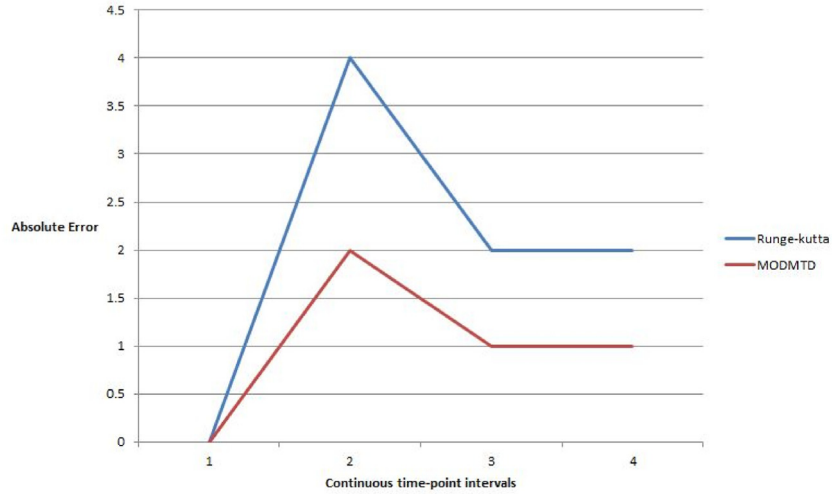

Fig. 9. The Absolute error rates for ModMTD and Runge-Kutta at low rain.

4. Discussion

The simulation results as depicted in the graphs showed that the predicted simulation values for variables $T, S, E, I, R, D, V, A, B \geq 0$ at all different time variants. Hence, the positivity proof of the model compartmental variables were in line with the model simulation results. The predicted malaria data were the future trends of the various variables $T, S, E, I, R, D, V, A, B$ in the system simulated for 1, 15, 30, 45, 60, 75, 90, 105 and 120 days.

Specifically, this study was more concerned about the I variable because it is the only variable whose simulated output can be validated against hospital-observed malaria incidences. Furthermore based on the model's prediction, malaria infected cases were highest during the heavy rainfall periods. Reason for the high rate of malaria during the heavy rain season was as a result of the high survival and reproduction rate of *Anopheles* spp during this period. Furthermore, the high survival and reproduction rate of *An. spp* was as a result of the increase in availability of stagnant water bodies during the rainy season (Arambepola et al., 2022).

In line with this, this study investigated the impact of potential malaria control strategies on malaria transmission dynamics. At 80% assumed vigilance to the use of traditional and conventional malaria control strategies during the two major seasons, malaria infection rate decreased when compared to the malaria infection simulation results obtained using the

acquired vigilant and susceptible data. At 98% assumed vigilance to the use of the malaria control strategies of interest in this work, the rate of malaria infection decreased most significantly during the dry season (low rainy peiod). The reason for the decrease in the malaria infection is as a result of decrease in the malarial vector population during the dry season. This was as a result of the decrease in the availability of stagnant water bodies. Although at 98% assumed vigilance initial condition at the two major different climatic scenarios, malaria importation still has significant impact on malaria transmission dynamics. Hence, it was opined that total vigilance to the use of LLIN, IRS, air conditioner, protective clothing, house net and lotion would be the most effective control strategy against malaria importation.

In order to further evaluate the performance of our model, this work showed that the simulation outputs from the novel algorithmic (ModMTD) implementation were relatively better in terms of model's prediction accuracy than the existing Runge-Kutta approach. This wa because the ABS_{error}, REL_{ERROR}, PER_{ERROR}, MSE and RMSE were smaller when the ModMTD was implemented in contrast to the aforementioned error values when the Runge-Kutta Numerical Solution method was used.

5. Conclusions

In this work, malaria transmission dynamics was studied using Covenant University in Nigeria as case study. The pilot population of interest in the study were the undergraduate students as a result of the ease of tracking their mobility. In line with this, a novel ODE-based mathematical models of malaria transmission dynamics incorporating human mobility as well as traditional and conventional control was developed based on the mass action and conservation principle. Different assumed vigilant conditions were tested in order to ascertain their efficacy in wiping out malaria. This study showed that at 98% best model-fit assumed vigilance condition, malaria importation still has a significant impact on malaria transmission dynamics at different seasonal scenarios. As a result of this, this study opined that total vigilance to usage of conventional and traditional malaria control strategies would be the most effective control against malaria.

This study is limited as it applied only hospital-reported imported malaria cases in the developed model. Local and global stability analyses of the equilibrium states of the model can be done in future studies. Sensitivity, bifurcation, and optimal control analyses of the model can also be done in future work. Further studies can also include other demographic parameters such as natural death and birth rates. Other modeling techniques such as the use of PDEs could be applied so as to include other heterogeneous factors such as age, gender, and race. With realistic parametric combinations, the novel model can be applied towards the control of other infectious diseases such as dengue, chikungunya, lassa fever among others.

Funding

This work was funded by the National Institutes of Health Common Fund [Grant no: 1U2RTW010679] under the West African Sustainable Leadership and Innovation Training in Bioinformatics Research Project and the World Bank (2019–2024). The funders had no role in study design, data collection and analysis, decision to publish, or preparation of the manuscript.

Data availabiliy

The novel malaria simulation tool developed in this work is available online via http://www.mbmpsdynamics.infinityfreeapp.com and its source codes are available on https://github.com/GbengaAdegbite/MalariaPredictionApp.

Authors contribution

Gbenga Adegbite: first draft writing, review, editing, conceptualization, methodology, data acquisition, software; Sunday Edeki: methodology, review and editing; Itunuoluwa Isewon: review and editing, Jerry Emmanuel:review and editing; Titilope Dokunmu:review and editing; Solomon Rotimi:review and editing; Jelili Oyelade: conceptualization, review, editing, methodology and supervision; Ezekiel Adebiyi:conceptualization and supervision.

Declaration of competing interest

The authors declare that there are no competing interest.

Acknowledgments

We acknowledge the support of Covenant University and Covenant Applied Informatics and Communications-African Centre of Excellence. The authors also acknowledged the constructive comments by the anonymous reviewers as well as Dr Godwin Oghonyon of the Department of Mathematics, Covenant University for further improving on the quality of the manuscript.

Appendix A. Supplementary data

Supplementary data to this article can be found online at https://doi.org/10.1016/j.idm.2023.08.005.

References

Abell, L. M., & Braselton, J. P. (2022). *Differential equations with mathematica*. Elsevier. https://www.elsevier.com/books/differential-equations-with-mathematica/abell/978-0-12-824160-8.

Achieng, E., Otieno, V., & Mung'atu, J. (2020). Modeling the trend of reported malaria cases in Kisumu county, Kenya. *F1000Research, 9*(1), 600.

Adeboye, N. O., Abimbola, O. V., & Folorunso, S. O. (2020). Malaria patients in Nigeria: Data exploration approach. *Data in Brief, 28*(1), Article 104997.

Adegbite, G., Edeki, S., Isewon, I., Dokunmu, T., Rotimi, S., Oyelade, J., & Adebiyi, E. (2022). Investigating the epidemiological factors responsible for malaria transmission dynamics. *IOP Conference Series: Earth and Environmental Science, 993*, Article 012008.

Adeola, A. M., Botai, J. O., Rautenbach, H., Adisa, O. M., Ncongwane, K. P., Botai, C. M., & Adebayo-Ojo, T. C. (2017). Climatic variables and malaria morbidity in mutale local municipality, South Africa: A 19-year data analysis. *International Journal of Environmental Research and Public Health, 14*(11), 1360.

Ahkrizal, A., Jaharuddin, J., & Nugrahani, E. H. (2023). Dynamics system in the SEIR- SI model of the spread of malaria with recurrence. *Jambura Journal of Biomathematics (JJBM), 4*(1), 31–36.

Ahmed, N., Shahid, N., Iqbal, Z., Jawaz, M., Rafiq, M., Tahira, S. S., & Ahmad, M. O. (2018). Numerical modeling of SEIQV epidemic model with saturated incidence rate. *J. Appl. Environ. Biol. Sci., 8*(4), 67–82.

Alegana, V. A., Khazenzi, C., Akech, S. O., & Snow, R. W. (2020). Estimating hospital catchments from in-patient admission records: A spatial statistical approach applied to malaria. *Scientific Reports, 10*(1), 1.

Almeida, R., Martins, N., & Silva, C. J. (2021). Global stability condition for the disease-free equilibrium point of fractional epidemiological models. *Axioms, 10*(4), 238.

Amambua-Ngwa, A., Amenga-Etego, L., Kamau, E., Amato, R., Ghansah, A., Golassa, L., Randrianarivelojosia, M., Ishengoma, D., Apinjoh, T., Maïga-Ascofaré, O., & Andagalu, B. (2019). Major subpopulations of *Plasmodium falciparum* in sub- saharan Africa. *Science, 365*(1), 813–816.

Anokye, R., Acheampong, E., Owusu, I., & Isaac, E. (2018). Time series analysis of malaria in Kumasi: Using ARIMA models to forecast future incidence. *Cogent social sciences, 4*(1), Article 1461544.

Arambepola, R., Lucas, T. C., Nandi, A. K., Gething, P. W., & Cameron, E. (2022). A simulation study of disaggregation regression for spatial disease mapping. *Statistics in Medicine, 41*(1), 1–16.

Awine, T., Malm, K., Bart-Plange, C., & Silal, S. P. (2017). Towards malaria control and elimination in Ghana: Challenges and decision making tools to guide planning. *Global Health Action, 10*(1), Article 1381471.

Badshah, N., & Akbar, H. (2021). Stability analysis of fractional order SEIR model for malaria disease in Khyber Pakhtunkhwa. *Demonstratio Mathematica, 54*(1), 326–334.

Bazan, M. J., & Mora, C. F. (2020). Compliance with preventive measures against malaria of personnel treated in the centre of international vaccination of the Minister of Defence (Spain). *Revista Española de Quimioterapia, 33*(1), 11.

Beier, J. C., Wilke, A. B., & Benelli, G. (2018). *Newer approaches for malaria vector control and challenges of outdoor transmission. Towards malaria elimination—a leap forward*. IntechOpen.

Benelli, G., & Beier, J. C. (2017). Current vector control challenges in the fight against malaria. *Acta Tropica, 174*(1), 91–96.

Bond, M. (2009). *Convolutions and the Weierstrass approximation theorem*. https://bondmatt.files.wordpress.com/2009/06/weierstrass.pdf.

Brauer, F. (2017). Mathematical epidemiology: Past, present, and future. *Infectious Disease Modelling, 2*(2), 113–127.

Buonomo, B., Chitnis, N., & d'Onofrio, A. (2018). Seasonality in epidemic models: A literature review. *Ricerche di Matematica, 67*(1), 7–25.

Chang, H. H., Wesolowski, A., Sinha, I., Jacob, C. G., Mahmud, A., Uddin, D., Zaman, S. I., Hossain, M. A., Faiz, M. A., Ghose, A., & Sayeed, A. A. (2019). Mapping imported malaria in Bangladesh using parasite genetic and human mobility data. *Elife, 8*(1), Article e43481.

Chutiman, N., Guayjrempanishk, P., Chiangpradit, M., Busababodhin, P., Rattanawan, S., & Kong-led, B. (2021). The forecasting model with climate variables of the Re- emerging disease rate in elderly patients. *WSEAS Transactions on Environment and Development, 17*(1), 866–875.

Collins, O. C., & Duffy, K. J. (2022). A mathematical model for the dynamics and control of malaria in Nigeria. *Infectious Disease Modelling, 7*(4), 728–741.

Darteh, E. K., Dickson, K. S., Ahinkorah, B. O., Owusu, B. A., Okyere, J., Salihu, T., Bediako, V., Budu, E., Agbemavi, W., Edjah, J. O., & Seidu, A. A. (2021). Factors influencing the uptake of intermittent preventive treatment among pregnant women in sub-saharan Africa: A multilevel analysis. *Archives of Public Health, 79*(1), 1–9.

Degarege, A., Fennie, K., Degarege, D., Chennupati, S., & Madhivanan, P. (2019). Improving socioeconomic status may reduce the burden of malaria in sub saharan Africa: A systematic review and meta-analysis. *PLoS One, 14*(1), Article e0211205.

Edeki, S. O., Adinya, I., Adeosun, M. E., & Ezekiel, I. D. (2020). Mathematical analysis of the global COVID-19 spread in Nigeria and Spain based on SEIRD model. *Commun. Math. Biol. Neurosci., 84*(1), 1–10.

Esayas, E., Tufa, A., Massebo, F., Ahemed, A., Ibrahim, I., Dillu, D., Bogale, E. A., Yared, S., & Deribe, K. (2020). Malaria epidemiology and stratification of incidence in the malaria elimination setting in Harari Region. *Eastern Ethiopia. Infectious Diseases of Poverty, 9*(1), 1–2.

Fischer, P. R. (2021). Emerging options for malaria prevention. *Infectious Disease Alert, 41*(1), 1–6.

Girum, T., Shumbej, T., & Shewangizaw, M. (2019). Burden of malaria in Ethiopia, 2000-2016: Findings from the global health estimates 2016. *Trop Dis Travel Med Vaccines, 5*(1), 11.

Guerra, C. A., Kang, S. Y., Citron, D. T., Hergott, D. E., Perry, M., Smith, J., Phiri, W. P., Nfumu, J. O., Eyono, J. N., Battle, K. E., & Gibson, H. S. (2019). Human mobility patterns and malaria importation on Bioko Island. *Nature Communications, 10*(1), 1–10.

Handari, B. D., Amalia, A., Rahmayani, A. S., & Aldila, D. (2020). Numerical simulation of malaria transmission model considering secondary infection. *Commun. Math. Biol. Neurosci., 36*(1), 1–10.

Herdicho, F. F., Chukwu, W., & Tasman, H. (2021). An optimal control of malaria transmission model with mosquito seasonal factor. Article *Results in Physics, 25*, Article 104238.

Imaga, O. F., Iyase, S. A., & Ogunniyi, P. O. (2022). Existence results for an m-point mixed fractional-order problem at resonance on the half-line. *Axioms, 11*, 630.

Inaba, H. (2017). Age-structured population dynamics in demography and epidemiology. *Springer Singapore, 1*(1), 10–20.

Iqbal, J., Al-Awadhi, M., & Ahmad, S. (2020). Decreasing trend of imported malaria cases but increasing influx of mixed *P. falciparum* and *P. vivax* infections in malaria-free Kuwait. *PLoS One, 15*(12), Article e0243617.

Kaindoa, E. W., Mmbando, A. S., Shirima, R., Hape, E. E., & Okumu, F. O. (2021). Insecticide-treated eave ribbons for malaria vector control in low-income communities. *Malaria Journal, 20*(1), 1–2.

Killeen, G. F., Tatarsky, A., Diabate, A., Chaccour, C. J., Marshall, J. M., Okumu, F. O., Brunner, S., Newby, G., Williams, Y. A., Malone, D., & Tusting, L. S. (2017). Developing an expanded vector control toolbox for malaria elimination. *BMJ Global Health, 2*(2), Article e000211.

Kojom, L. P., & Singh, V. (2020). Prevalence of Plasmodium falciparum field isolates with deletions in histidine-rich protein 2 and 3 genes in context with sub-saharan Africa and India: A systematic review and meta-analysis. *Malaria Journal, 19*(1), 1–4.

Krezanoski, P. J., Bangsberg, D. R., & Tsai, A. C. (2018). Quantifying bias in measuring insecticide-treated bednet use: meta-analysis of self-reported vs objectively measured adherence. *Journal of global health, 8*(1), 1–10.

Li, Y., & Liu, X. (2020). Modeling and control of mosquito-borne diseases with Wolbachia and insecticides. *Theoretical Population Biology, 132*(1), 82–91.

Marshall, J. M., Wu, S. L., Kiware, S. S., Ndhlovu, M., Ouédraogo, A. L., Touré, M. B., Sturrock, H. J., Ghani, A. C., & Ferguson, N. M. (2018). Mathematical models of human mobility of relevance to malaria transmission in Africa. *Scientific Reports, 8*(1), 1–2.

Mekuriaw, W., Yewhalaw, D., Dugassa, S., Taffese, H., Bashaye, S., Nigatu, W., & Massebo, F. (2020). Distribution and trends of insecticide resistance in malaria vectors in Ethiopia (1986-2017): A review. *Ethiopian Journal of public health and nutrition, 3*(Special), 51.

Mukhtar, A. Y., Munyakazi, J. B., & Ouifki, R. (2020). Assessing the role of human mobility on malaria transmission. *Mathematical Biosciences, 320*(1), Article 108304.

N'Do, S., Bandibabone, J. B., Soma, D. D., Musaka, B. Z., Prudhomme, J., Habamungu, C. C., Namountougou, M., Sangaré, I., Kientega, M., Kaboré, D. A., & Bayili, K. (2021). Insecticide resistance profiles in malaria vector populations from Sud- Kivu in the Democratic Republic of the Congo. *Transactions of the Royal Society of Tropical Medicine & Hygiene, 115*(11), 1339–1344.

Nana-Kyere, S., Doe, R. H., Boateng, F. A., Odum, J. K., Marmah, S., & Banon, D. T. (2017). Optimal control model of malaria disease with standard incidence rate. *Journal of Advances in mathematics and Computer Science, 1*(1), 1–21.

Narain, J. P., & Nath, L. M. (2018). Eliminating malaria in India by 2027: The countdown begins. *Indian Journal of Medical Research, 148*(2), 123.

Ndipmong, U., & Udechukwu, P. (2022). Analysis of numerical methods for solving first order non-linear differential equations. *Asian Journal of Pure and Applied Mathematics, 4*(1), 414–424.

Ngandu, C. B., Momberg, D., Magan, A., Chola, L., Norris, S. A., & Said-Mohamed, R. (2020). The association between household socio-economic status, maternal socio-demographic characteristics and adverse birth and infant growth outcomes in sub-saharan Africa: A systematic review. *Journal of developmental origins of health and disease, 11*(4), 317–334.

Ngninpogni, D. M., Ndo, C., Akono, P. N., Nguemo, A., Nguepi, A., Metitsi, D. R., Tombi, J., Awono-Ambene, P., & Bilong, C. F. (2021). Insights into factors sustaining persistence of high malaria transmission in forested areas of sub-saharan Africa: The case of mvoua, south Cameroon. *Parasites & Vectors, 14*(1), 1–10.

Nkiruka, O., Prasad, R., & Clement, O. (2021). Prediction of malaria incidence using climate variability and machine learning. *Informatics in Medicine Unlocked, 22*(1), Article 100508.

Oghonyon, G. J., Okunuga, S. A., & Ogunniyi, P. O. (2022). An efficient block solver of trigonometrically fitted method for stiff ODEs. *Advances in Differential Equations and Control Processes, 28*(1), 73–98.

Okuneye, K., & Gumel, A. B. (2017). Analysis of a temperature-and rainfall-dependent model for malaria transmission dynamics. *Mathematical Biosciences, 287*, 72e92.

Omoloye, M. A., Udokang, A. E., Sanusi, A. O., & Emiola, O. K. (2022). Analytical solution of dynamical transmission of Malaria disease model using differential transform method. *Int. J. Novel Res. Phys. Chem. Math., 9*(1), 1–13.

Porter, T. R., Finn, T. P., Silumbe, K., Chalwe, V., Hamainza, B., Kooma, E., Moonga, H., Bennett, A., Yukich, J. O., Steketee, R. W., & Keating, J. (2020). Recent travel history and *Plasmodium falciparum* malaria infection in a region of heterogenous transmission in Southern Province, Zambia. *The American Journal of Tropical Medicine and Hygiene, 103*(2), 74.

Ryan, S. J., Martin, A. C., Walia, B., Winters, A., & Larsen, D. A. (2020). Comparing prioritization strategies for delivering indoor residual spray (IRS) implementation, using a network approach. *Malaria Journal, 19*(1), 1–9.

Schwinning, S., Sala, O. E., Loik, M. E., & Ehleringer, J. R. (2004). Thresholds, memory, and seasonality: Understanding pulse dynamics in arid/semi-arid ecosystems. *Oecologia, 141*, 191–193.

Shellvarajah, M., Hatz, C., & Schlagenhauf, P. (2017). Malaria prevention recommendations for risk groups visiting sub-saharan Africa: A survey of European expert opinion and international recommendations. *Travel Medicine and Infectious Disease, 19*(1), 49–55.

Sweilam, N. H., Al-Mekhlafi, S. M., Mohammed, Z. N., & Baleanu, D. (2020). Optimal control for variable order fractional HIV/AIDS and malaria mathematical models with multi-time delay. *Alexandria Engineering Journal, 59*(5), 3149–3162.

Syme, T., Fongnikin, A., Todjinou, D., Govoetchan, R., Gbegbo, M., Rowland, M., Akogbeto, M., & Ngufor, C. (2021). Which indoor residual spraying insecticide best complements standard pyrethroid long-lasting insecticidal nets for improved control of pyrethroid resistant malaria vectors? *PLoS One, 16*(1), Article e0245804.

Tchoumi, S. Y., Kouakep, Y. T., Fotsa, D. J., Kamba, F. G., Kamgang, J. C., & Houpa, D. D. (2021). Mathematical model for acquiring immunity to malaria: A PDE approach. *Bio-Mathematics, 10*(2), Article 2107227.

Weiss, D. J., Lucas, T. C., Nguyen, M., Nandi, A. K., Bisanzio, D., Battle, K. E., Cameron, E., Twohig, K. A., Pfeffer, D. A., Rozier, J. A., Gibson, H. S., et al. (2019). Mapping the global prevalence, incidence, and mortality of *Plasmodium falciparum*, 2000–17: A spatial and temporal modelling study. *The Lancet, 394*, 322–331.

World Health Organization. (2018). High burden to high impact. . *A targeted malaria response, 1*, 1–5. https://apps.who.int/iris/bitstream/handle/10665/275868/WHO- CDS-GMP-2018.25-eng.pdf.

World Health Organization. (2020). The potential impact of health service disruptions on the burden of malaria: A modelling analysis for countries in sub-saharan Africa. *Global Malaria Programme, 1–8*. https://apps.who.int/iris/bitstream/handle/10665/331845/9789240004641-eng.pdf.

Yamana, T. K., Qiu, X., & Eltahir, E. A. (2017). Hysteresis in simulations of malaria transmission. *Advances in Water Resources, 108*, 416–422.